methyl and meso-H. Thus, it is not surprising that 4-Ac-deuterohemin has the same orientation as found for 4-V-deuterohemin, while 2-Ac-deuterohemin displays heme disorder similar to that of 2-V-deuterohemin, with the major compound possessing the same reversed orientation (B in Figure 1). Acetyl resonances are not resolved in any low-spin ferric complex. Unfortunately, the significantly reduced stability of compound I for acetyl derivatives of HRP precludes detection of their ^1H NMR spectra.

Thus, we conclude that determination of the influence peripheral substituents have on the porphyrin orientation in b-type low-spin ferric hemoproteins using our NMR method[13] may provide a general technique for detailed characterization of heme-protein interactions. We further conclude that the heme–protein steric interactions which tend to force the 2 substituent into the heme plane are primarily responsible for determining the orientation of the heme in the heme pocket of HRP. A possible functional role of the steric clamping is suggested to be stabilization of the porphyrin cation radical of the compound by extension of the π system to the vinyl group.

Acknowledgment. This research was supported by grants from the National Institutes of Health, Grants HL-16087, HL-22252, and GM-26226.

Registry No. HRP, 9003-99-0; heme, 14875-96-8; 2-Ac-deuterohemin, 68866-16-0; 2-V-deuterohemin, 78694-18-5; 4-Ac-deuterohemin, 68949-21-3; 4-V-deuterohemin, 78694-17-4; 2,4-Ac_2-deuterohemin, 14977-95-8; deuterohemin, 21007-21-6.

Chemistry, Spectroscopy, and Isotope-Selective Infrared Photochemistry of a Volatile Uranium Compound Tailored for 10-μm Absorption: $U(OCH_3)_6$

Edward A. Cuellar, Steven S. Miller, Tobin J. Marks,*[1a] and Eric Weitz*[1b]

Contribution from the Department of Chemistry and the Materials Research Center, Northwestern University, Evanston, Illinois 60201. *Received July 19, 1982*

Abstract: This contribution reports on the chemical, vibrational spectroscopic, and infrared multiphoton photochemical properties of uranium hexamethoxide, $U(OCH_3)_6$, a prototype molecule for laser-induced uranium isotope separation with a carbon dioxide laser. Uranium hexamethoxide can be prepared from UCl_4 by conversion to $Li_2U(OCH_3)_6$, followed by oxidation with lead tetraacetate. Vapor pressure studies on $U(OCH_3)_6$ indicate that $\Delta H_{sub}^\circ = 23 \pm 3$ kcal/mol and $\Delta S_{sub}^\circ = 76 \pm 4$ eu; at 33 °C, the vapor pressure is 17 mtorr. The vibrational spectra of $U(^{16}OCH_3)_6$ and $U(^{18}OCH_3)_6$ have been assigned by using infrared and laser Raman data. Under idealized O_h symmetry, the $U(^{16}OCH_3)_6$ U–O stretching fundamentals are assigned at 505.0 (A_{1g}), 464.8 (T_{1u}), and 414.0 cm^{-1} (E_g). Tentative assignments are also made for several of the overtone and combination transitions evidence for possible lowering of the symmetry is presented. In gas-phase infrared photochemical experiments, the predominant $U(OCH_3)_6$ photoproducts isolated are $U(OCH_3)_5$, methanol, and formaldehyde. These are suggestive of multiphoton U–O bond homolysis to produce uranium pentamethoxide and methoxy radicals. The enrichment of unreacted $U(OCH_3)_6$ in ^{235}U is maximum at ca. 927 cm^{-1} (near what may be a U–O stretching overtone transition) and exhibits both a low fluence threshold and diminution at high fluence.

Introduction

The efficient separation of isotopes by selective laser-induced multiphoton infrared excitation of polyatomic molecules is now an experimental reality as well as a subject of considerable current theoretical interest.[2] A wide variety of systems have been studied, and laboratory-scale isotope separation has been achieved for a host of elements including hydrogen,[2,3] boron,[4] carbon,[4b,5] oxygen,[6] silicon,[4b] sulfur[2,7] chlorine,[8] molybdenum,[9a] selenium,[9b] and osmium.[10] The key molecular requirements for any efficient laser-induced isotope separation process employing polyatomic molecules include (i) volatility, preferably approaching ca. 1 torr at ambient temperatures (operating pressures appreciably in excess of this are likely a disadvantage), (ii) the existence of an infrared-active normal vibrational mode (fundamental, overtone, or combination) that exhibits a nonzero isotope shift and absorbs in the spectral region corresponding to the output of an efficient laser system, (iii) the absence of interfering ligand absorptions, (iv) the ready synthesis of large quantities of the target molecule, (v) the facile separation and recycling of enriched and depleted material, and (vi) the absence of undesirable photochemical side reactions such as nonselective photodecomposition.

In practice, the isotope-sensitive transition of the target molecule is brought into resonance or near resonance in the gas phase with a high fluence infrared laser source. The result is isotope-selective

(1) (a) Camille and Henry Dreyfus Teacher–Scholar. (b) Alfred P. Sloan Fellow.

(2) (a) Steinfeld, J. I. "Laser Induced Chemical Processes"; Plenum Press: New York, 1981. (b) Schulz, P. A.; Subdø, A. S.; Krajnovich, D. J.; Kwok, H. S.; Shen, Y. R.; Lee, Y. T. *Annu. Rev. Phys. Chem.* **1979**, *30*, 379. (c) Letokhov, V. S. *Nature (London)* **1979**, *277*, 605. (d) Cantrell, C. D.; Freund, S. M.; Lyman, J. L. In "Laser Handbook"; North-Holland Publishing Co.: Amsterdam, 1978; Vol. III. (e) Letokhov, V. S.; Moore, C. B. In "Chemical and Biological Applications of Lasers"; Moore, C. B., Ed.; Academic Press: New York, 1977; Vol. III, pp 1–165. (f) Letokhov, V. S. *Annu. Rev. Phys. Chem.* **1977**, *28*, 133.

(3) Koren, G.; Oppenheim, U. P.; Tal, D.; Okon, M.; Weil, R. *Appl. Phys. Lett.* **1976**, *29*, 40.

(4) (a) Ambartzumian, R. V.; Letokhov, V. S.; Ryabov, E. A.; Chekalin, N. V. *JETP Lett. (Engl. Transl.)* **1974**, *20*, 273. (b) Lyman, J. L.; Rockwood, S. D. *J. Appl. Phys.* **1976**, *47*, 595.

(5) (a) Yogev, A.; Benmair, R. M. J. *Chem. Phys. Lett.* **1979**, *63*, 558. (b) Bittenson, S.; Houston, P. L. *J. Chem. Phys.* **1977**, *67*, 4819. (c) Ritter, J. J.; Freund, S. M. *J. Chem. Soc., Chem. Commun.* **1976**, 811.

(6) Cox, D. M.; Hall, R. B.; Horsley, J. A.; Kramer, G. M.; Rabinowitz, P.; Kaldor, A. *Science (Washington, D.C.)* **1979**, *No. 205*, 390.

(7) (a) Ambartsumian, R. V.; Gorokhov, Y. A.; Letakhov, V. S.; Makarov, G. N. *JETP Lett., (Engl. Transl.)* **1975**, *21*, 171–172. (b) Lyman, J. L.; Jensen, R. J.; Robinson, C. P. *Appl. Phys. Lett.* **1975**, *27*, 87–89.

(8) (a) Ambartzumian, R. V.; Gorokhov, Y. A.; Letokhov, V. S.; Makarov, G. N.; Puretzky, A. A. *Phys. Lett. A* **1976**, *56A*, 183. (b) Lamotte, M.; Dewey, H. J.; Keller, R. A.; Ritter, J. J. *Chem. Phys. Lett.* **1975**, *30*, 165.

(9) (a) Freund, S. M.; Lyman, J. L. *Chem. Phys. Lett.* **1978**, *55*, 435. (b) Tiee, J. J.; Wittig, C. *Appl. Phys. Lett.* **1978**, *32*, 236.

(10) (a) Ambartzumian, R. V.; Letokhov, V. S.; Makarov, G. N.; Puretzky, A. A. *Opt. Commun.* **1978**, *25*, 69. (b) Ambartzumian, R. V.; Gorokhov, Yu. A.; Letokhov, V. S.; Makarov, G. N. *JETP Letters (Engl. Transl.)* **1975**, *22*, 43.

0002-7863/83/1505-4580$01.50/0

decomposition or, in the presence of appropriate reagents, isotope-selective reaction. Alternative photochemical excitation sequences have included two infrared sources tuned to slightly different frequencies[2,11] and combined infrared–UV excitation.[2] In ideal cases, the isotopically enriched (or depleted) photoproduct is easily separated from starting materials on the basis of such physical properties as volatility or solubility, although in many laboratory-scale experiments this has not been attempted. To date, most laser-induced multiphoton isotope separation (MIS) studies have employed pulsed, discretely tunable, CO_2 infrared gas lasers. Such devices have a usable output in the 10-μm region (9.2–10.8 μm) and are by far the most powerful, reliable, and economical sources of midinfrared radiation presently available.

In principle, multiphoton infrared photochemistry would appear to be an attractive approach to the technologically important (and currently highly energy intensive) enrichment of natural uranium (^{235}U, 0.72% natural abundance; ^{238}U, 99.27% natural abundance[12]) or of diffusion/centrifuge-derived uranium tailings to the ca. 3% ^{235}U level required for fissile fuel.[2,13–19] However, detailed spectroscopic studies indicate that the initially most attractive candidate for a molecular process, UF_6, lacks significant absorption in the output region of the CO_2 gas laser.[14,20] Since UF_6 does possess suitable vibrational transitions in the 16-μm region, intense effort has been directed toward the development of efficient and reliable 16-μm laser sources for UF_6 infrared photochemistry.[21,22] Although such activities may eventually bear fruit, an attractive and challenging alternative approach would be to "tailor" volatile uranium molecules for isotope-sensitive absorption in the 10-μm region.[23] We recently communicated our initial spectroscopic and photochemical observations on the prototype molecule uranium hexamethoxide, $U(OCH_3)_6$.[24] With a relatively simple CO_2 laser irradiation system, it was possible to achieve significant uranium isotope enrichment in this volatile uranium–organic molecule. Subsequent, complementary studies with a CO_2 laser have achieved similar results in a molecular beam of either of two uranyl β-diketonate compounds.[6,25,26] Infrared photolysis of volatile $U(BD_4)_4$[27] does not appear to result in uranium isotope enrichment under the conditions employed.[28]

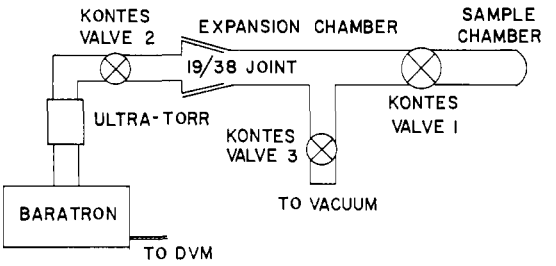

Figure 1. Schmeatic drawing of apparatus for measuring $U(OCH_3)_6$ vapor pressures.

In the present contribution we present a detailed discussion of the chemical, physical, spectroscopic, and photophysical properties of $U(OCH_3)_6$ as regards the amenability to and mechanism of uranium isotope selective multiphoton infrared photochemistry. In parallel contributions, we discuss additional approaches to the synthesis of $U(OCH_3)_6$ and related compounds,[29] as well as further information on molecular[30] and electronic[29,31] structure.

Experimental Section

Materials Preparation and Handling. All sample manipulations and preparations were carried out either under high vacuum on a grease-free vacuum line or under an atmosphere of prepurified nitrogen, using standard vacuum line and Schlenk techniques and a Vacuum Atmospheres Corp. HE-43-2 Dri-Lab glovebox fitted with a HE-193-1 Dri-Train atmosphere recirculating unit. All solvents were freshly distilled under an atmosphere of prepurified nitrogen from the appropriate drying agents.[32] Anhydrous uranium tetrachloride was prepared by the literature procedure,[33] and $H_2{}^{18}O$ (≥97% ^{18}O) was purchased from Yeda Research and Development, Rehovot, Israel.

$U(OCH_3)_6$ Synthesis. Uranium hexamethoxide was prepared from UF_6 by the procedure described elsewhere[29] or from anhydrous UCl_4 as described below.

To a 500-mL three-necked flask containing 150 mL of dry methanol was added 6.6 g (0.79 mol) lithium wire. The mixture was stirred under a nitrogen blanket until a clear solution was obtained. To the clear

(11) Ambartzumian, R. V.; Letokhov, V. S. In "Chemical and Biochemical Applications of Lasers"; Moore, C. B., Ed.; Academic Press: New York, 1977; Vol. III, pp 167–316.
(12) Lederer, C M., Shirley, V. S., Eds. "Table of Isotopes", 7th ed.; Wiley-Interscience: New York, 1978; p 1443.
(13) For general overviews see: (a) Villani, S. *Top. Appl. Phys.* **1979**, *35*, 1. (b) Plurien, P. L.; Mezin, M. M. *AIChE Symp. Ser.* **1977**, *No. 169*, 15. (c) Vanstrum, P. R.; Wilcox, W. J., Jr. *Ibid.* **1977**, *No. 169*, 83.
(14) Reviews of laser processes: Lester, R. K. *Technol. Rev.* **1980**, *82*, 18 and references therein. Jensen, R. J.; Judd, O'D. P.; Sullivan, J. A. *Los Alamos Science* **1982**, *3*, 2–33.
(15) Review of the gaseous diffusion process: Massignon, D. *Top. Appl. Phys.* **1979**, *35*, 55.
(16) Reviews of the gas centrifuge process: Von Halle, E. *AIChE Symp. Ser.* **1980**, *No. 192*, 82 and references therein.
(17) Reviews of various aerodynamic processes: Anderson, J. B. *AIChE Symp. Ser.* **1980** *No. 192*, 89 and references therein.
(18) Review of chemical separation processes: Laskorin, B. N.; Babenko, A. M.; Filippov, E. A.; Trubnikov, A. F. *Russ. Chem. Rev.* (*Engl. Transl.*) **1975**, *44*, 381.
(19) Review of plasma separation techniques: Boeschoten, F.; Nathrath, N. *Top. Appl. Phys.* **1979**, *35*, 291.
(20) (a) Cox, D. M.; Elliott, J. *Spectros. Lett.* **1979**, *12*, 275. (b) Erkens, J. W. *Appl. Phys.* **1976**, *10*, 15. (c) Paine, R. T.; McDowell, R. S.; Asprey, L. B.; Jones, L. H. *J. Chem. Phys.* **1976**, *64*, 3081. (d) McDowell, R. S.; Asprey, L. B.; Paine, R. T. *Ibid.* **1974**, *61*, 3571.
(21) (a) Suzuki, K.; Saito, S.; Obara, M.; Fujioka, T. *J. Appl. Phys.* **1980**, *51*, 4003 and references therein. (b) Gürs, K.; Hofmann, H.; Schäfer, G. *Opt. Commun.* **1980**, *33*, 197; (c) *Laser Focus* (*Fiberoptic Commun.*) **1980**, *16*, 20. (d) Wexler, B. L.; Waynant, R. W. *Appl. Phys. Lett.* **1979**, *34*, 674. (e) Rabinowitz, P.; Stein, A.; Brickman, R.; Kaldor, A. *Ibid.* **1979**, *35*, 739. (f) Tiee, J. J.; Fischer, T. A.; Wittig, C. *Rev. Sci. Instrum.* **1979**, *50*, 958. (g) Tiee, J. J.; Wittig, C. *J. Appl. Phys.* **1978**, *49*, 61; (h) *Laser Focus* (*Fiberopt. Commun.*) **1978**, *14*, 36. (i) Grischkowsky, D. R.; Lankard, J. R.; Sorokin, P. P. *IEEE J. Quantum Electron.* **1977**, *QE-13*, 392.
(22) (a) Horsley, J. A.; Rabinowitz, P.; Stein, A.; Cox, D. M.; Brickman, R. O.; Kaldor, A. *IEEE J. Quantum Electron.* **1980**, *QE-16*, 412. (b) Rabinowitz, P.; Stein, A.; Kaldor, A. *Opt. Commun.* **1978**, *27*, 381. (c) Tiee, J. J.; Wittig, C. *Ibid.* **1978**, *27*, 377; (d) *Laser Focus* (*Fiberopt. Commun.*) **1978**, *14*, 32.
(23) (a) Coleman, J. H.; Marks, T. J. *U.S. Patent* 4 097 384. (b) Cuellar, E. A.; Marks, T. J.; Miller, S. S.; Weitz, E. *U.S. Patent* 4 364 870.
(24) (a) Miller, S. S.; DeFord, D. D.; Marks, T. J.; Weitz, E. *J. Am. Chem. Soc.* **1979**, *101*, 1036. (b) Cuellar, E. A.; Miller, S. S.; Teitelbaum, R. C.; Marks, T. J.; Weitz, E. In "Progress in Rare Earth Science and Technology"; Silber, H. S., Rhyne, J. J. Eds.; Plenum Press: New York, 1982; Vol. III, pp 71–76. (c) Cuellar, E. A. Ph.D. Thesis, Northwestern University, 1981.
(25) (a) Cox, D. M.; Horsley, J. A. *J. Chem. Phys.* **1980**, *72*, 864. (b) Kaldor, A.; Hall, R. B.; Cox, D. M.; Horsley, J. A.; Rabinowitz, P.; Kramer, G. M. *J. Am. Chem. Soc.* **1979**, *101*, 4465. (c) Cox, D. M.; Maas, E. T., Jr. *Chem. Phys. Lett.* **1980**, *71*, 330. (d) The antisymmetric OUO stretching mode at ca. 950 cm^{-1} was irradiated.
(26) For other studies of β-diketonate compounds, including work bearing upon whether enriched products would actually be isolable via the process of ref 25, see: (a) Ekstrom, A.; Randall, C. H. *Inorg. Chem.* **1981**, *20*, 626–629 and references therein. (b) Ekstrom, A.; Loeh, H.; Randall, C. H.; Szego, L.; Taylor, J. C. *Inorg. Nucl. Chem. Lett.* **1978**, *14*, 301. (c) Ekstrom, A.; Randall, C. H. *J. Phys. Chem.* **1978**, *82*, 2180. (d) Taylor, J. C.; Ekstrom, A.: Randall, C. H. *Inorg. Chem.* **1978**, *17*, 3285. (e) Ekstrom, A.; Hurst, H. J.; Loeh, H.; Randall, C. H. *Chem. Phys. Lett.* **1982**, *86*, 7.
(27) (a) Schlesinger, H. I.; Brown, H. C. *J. Am. Chem. Soc.* **1953**, *75*, 219. (b) Bernstein, E. R.; Hamilton, W. C.; Keiderling, T. A.; LaPlaca, S. J.; Lippard, S. J.; Mayerle, J. J. *Inorg. Chem.* **1972**, *11*, 3009. (c) Volkov, V. V.; Myakishev, K. G. *Sov. Radiochem.* (*Engl. Transl.*) **1976**, *18*, 512. (d) Paine R. T.; Light, R. W.; Nelson, M. *Spectrochim. Acta, Part A* **1979**, *35A*, 213.
(28) (a) Paine, R. T.; Schonberg, P. R.; Light, R. W.; Danen, W. C.; Freund, S. M. *J. Inorg. Nucl. Chem.* **1979**, *41*, 1577. (b) A UD_3B bridge deformation mode (ref 28c) at 924 cm^{-1} was irradiated. There is evidence for ^{11}B enrichment. (c) Marks, T. J.; Kolb, J. R. *Chem. Rev.* **1977**, *77*, 263.
(29) (a) Cuellar, E. A.; Marks, T. J. *Inorg. Chem.* **1981**, *20*, 2129. (b) See also: Jacob, E. *Angew. Chem., Int. Ed. Engl.* **1982**, *21*, 142.
(30) Miller,, S. S.; Day, V. W.; Marks, T. J.; Weitz, E., manuscript in preparation.
(31) Miller, S. S.; Seyam, A. M.; Fragalà, I.; Marks, T. J.; Weitz, E., manuscript in preparation.
(32) P_2O_5 for CCl_4; sodium–benzophenone for THF, ethyl ether, toluene, and pentane; Mg for CH_3OH. (a) Vogel, A. I. "Textbook of Practical Organic Chemistry", 4th ed.; Furniss, B. S., Hannaford, A. J., Rogers, V., Smith, P. W. G., Tatchell, A. R., Eds.; Longman: London, 1978; pp 264–279. (b) Jolly, W. L. "The Synthesis and Characterization of Inorganic Compounds"; Prentice-Hall: Englewood Cliffs, NJ, 1970; pp 114–121.
(33) Hermann, J. A.; Suttle, J. F. *Inorg. Synth.* **1957**, *5*, 143.

solution was added 50 g (0.13 mol) UCl_4. An immediate formation of the light green precipitate, presumably lithium hexamethoxyuranate(IV) ($Li_2(U(OCH_3)_6)$), was observed. The excess solvent was removed from the light green suspension by trap-to-trap distillation at room temperature. The solid was then collected in the glove box, pulverized, and returned to the flask. Freshly distilled, dry THF (300 mL) was added to the flask and the mixture cooled to 0 °C in an ice bath. With vigorous stirring, 58.3 g (0.13 mol) of $Pb(O_2CCH_3)_4$ (Aldrich, previously washed with pentane and dried under high vacuum) was added. The green suspension gradually turned a deep red. The resultant mixture was next allowed to warm to room temperature over the course of 1 h and was then suction filtered under nitrogen in a Schlenk frit. The THF solvent was removed in vacuo, leaving a red solid, $U(OCH_3)_6$. To this red solid was added 300 mL of freshly distilled, dry pentane. The solution was again filtered and then slowly cooled to −120 °C (liquid nitrogen/pentane slush bath). The clear supernatant was removed via syringe and discarded. The residual crystalline solid was then dried in vacuo, yield 28 g (51%) of dark red, hexagonal plates. This material is identical with that prepared by alternative routes[29a] as confirmed by melting point as well as infrared and ^1H NMR spectroscopy. For spectroscopic and photochemical studies, this material was sublimed repeatedly at room temperature and at 10^{-5} torr onto a dry-ice-cooled cold finger with exclusion of room light. Uranium hexamethoxide was stored in the dark at −20 °C.

$U(^{18}OCH_3)_6$ Synthesis. By use of the published procedure,[29] oxygen-18 labeled uranium hexamethoxide, $U(^{18}OCH_3)_6$, was prepared from UF_6 and $Na^{18}OCH_3$, the $Na^{18}OCH_3$ being prepared from Na and $CH_3{}^{18}OH$[34] in dry THF. The isotopic purity of the $U(^{18}OCH_3)_6$ was determined by mass spectrometry; it was found that >92% of the methoxy ligands contained ^{18}O.

Vibrational Spectroscopy. Infrared spectra were acquired with either a Perkin-Elmer 283 grating infrared spectrometer or Nicolet 7199 FT IR (equipped with both triglycine sulfide (TGS) and HgCdTe detectors). Samples were studied as solutions in dry, degassed Nujol contained between KBr plates and held in airtight sample containers, as KBr pellets, as thin films, and as a gas in an 8.5-cm path length evacuable glass cell fitted with KBr windows and a side arm to contain the sample. Consecutive scans were made of each sample to check for possible decomposition in previous scans, and at the end of a series of scans, the samples were deliberately exposed to air to ascertain the effect on the spectrum. Raman spectra were acquired with 6471- (Spectra Physics, Kr^+) or 5145-Å (Spectra Physics, Ar^+) excitation with use of a Spex 1401 double monochromator, photon counting detection, and a spinning sample configuration. Solid samples were studied at −30 to −65 °C, and solution samples (in toluene) at 18 to −85 °C. In both cases, repetitive scans were made to check for possible decomposition in the laser beam.

Vapor Pressure Measurements. The vapor pressure of $U(OCH_3)_6$ was measured as a function of temperature in a Pyrex apparatus[24c] consisting of a sample chamber connected to an expansion chamber by a Teflon high-vacuum valve as shown in Figure 1. The expansion chamber in turn was connected, by Teflon valves, to an MKS-221A Baratron capacitance manometer and to a high-vacuum line. The entire apparatus could be contained in a light-proof, variable-temperature compartment consisting of a box equipped with an efficient fan and resistance heating tape. Temperature regulation to ±0.5 °C was achieved. The apparatus sample chamber was loaded with freshly purified, crystalline $U(OCH_3)_6$, was then evacuated to $<10^{-4}$ torr pressure, and was allowed to outgas for approximately 24 h. This procedure also removed any volatile impurities in the sample. The $U(OCH_3)_6$ was then allowed to equilibrate with its vapor in the volume defined by the sample chamber and the attached expansion chamber. This procedure was carried out to minimize the possible effect of any small leaks and of sample decomposition occurring due to contact between $U(OCH_3)_6$ vapor and the metal surface of the manometer. At each temperature, the equilibration times were varied from 5 up to 90 min. The valve between the sample compartment and expansion chamber (valve 1) was then closed, and the valve between the expansion chamber and the Baratron (valve 2) was opened and the pressure read in millivolts on a Data Precision 248 digital voltmeter. The vapor pressure of $U(OCH_3)_6$, P, was then calculated from eq 1. Here

$$P = \{(P_F - P_Z) - (P_1 - P_Z)(V_C/V_{B+C})\}(V_{B+C}/V_B) - P_L t \quad (1)$$

P_F is the final pressure measured when valve 2 is opened, P_1 is the pressure reading just before opening valve 2, P_Z is the zero reference reading taken when the entire system is under a dynamic vacuum of $<10^{-4}$ torr, V_B is the volume of the expansion chamber (16.6 cm^3), V_C is the volume between the pressure gauge and valve 2 (12.4 cm^3), t is the equilibration time in minutes, and P_L is the correction factor for the pressure increase per minute in the expansion chamber when it is entirely isolated (presumable due to slight outgassing/leakage of the Teflon valves). The variable P_L was evaluated by running a blank experiment (valve 1 to sample chamber closed) and setting $P = 0$ in eq 1. The value of P_F was recorded as soon as a stable reading was reached (ca. 5 s). The pressure began to slowly rise after this. Since there was outgassing, it was not possible to determine how much, if any, of this rise was due to sample decomposition. Typically, P_L was approximately 0.3 μm/min. These uncertainties did not affect the vapor pressure measurements since readings obtained after 16 min of equilibration were equal to those of 30–45 min once stable values were reached. Significantly longer equilibration times led to higher pressures, indicative of possible sample decomposition.

Infrared Photochemistry. Apparatus. Two infrared lasers were utilized in the irradiation studies of the $U(OCH_3)_6$. One was a home-built Rogowski profile CO_2 double-discharge TEA laser that produced pulses on the P(38) line of the 00^01-10^00 transition that varied in energy from 0.9 to 1.2 J/pulse. The repetition rate of this system was 1.0 Hz, and the pulse widths were typically 80 ns (full width at half maximum) with a low-intensity (30%) 500-ns tail. Alternatively, a commercial (Lumonics K 202-2) CO_2 laser was used that produced as much as 15 J/pulse on the P branch lines of the 00^01-10^00 transition in CO_2. The repetition rate for this system was also typically 1.0 Hz although the pulse width was somewhat greater than in the previously described home-built system. The output of this system was spatially filtered, and the maximum unfocused fluence after filtering was approximately 5.5 J/cm^2.

Laser lines were identified with an Optical Engineering CO_2 spectrum analyzer. Laser energies were measured with a calibrated Scientech calorimeter, and a photon drag detector was used to observe the temporal evolution of the laser pulse.

With either laser, the sample was irradiated in a 2.5-cm i.d. 42.0-cm path length cylindrical Pyrex cell fitted with KCl or KBr front windows. In the case of the home-built laser system, a rear reflector was used for double-passing the beam. With the commercial laser, the beam exited the cell through a KCl or KBr window. Sample containers were connected to either end of the evacuable irradiation cell. The unirradiated solid sample was placed in one compartment and the vapor was allowed to pass down the length of the cell, during which time it was irradiated. The vapor was continuously condensed in a liquid-nitrogen-cooled container on the opposite end of the cell. The collecting chamber consisted of a symmetric multifingered "carousel" manifold so that irradiated samples and blanks could be collected in separate, sealable containers for subsequent isotopic analysis without variation of the cell geometry. Irradiation fluences were calculated from the average of the energy entering and leaving the cell and from burn patterns on graph paper as measured at the cell windows.

Infrared Photochemistry. Procedure. The entire irradiation cell, except the sample reservoir, was evacuated to 10^{-5}–10^{-6} torr and flamed with a Bunsen burner. When cooled, the sample reservoir was opened and pumped to ca. 10^{-5} torr (the dynamic vapor pressure of the pumped system with the reservoir opened). Three of the four carousel collection compartments were closed off from the system, and the remaining compartment was immersed in liquid nitrogen. The valve to the vacuum system was then closed, and the cell was conditioned by allowing $U(OCH_3)_6$ (ca. 1 mg) to pass through the cell and condense as a red-orange ring in the collection compartment. This material also served as a source of unirradiated reference material during later mass spectrometric isotope analysis (vide infra).

After collection of the aforementioned reference sample, the collection compartment was warmed to ambient temperature, and the cell was briefly reevacuated to remove residual vapors formed during cell conditioning (presumably methanol). The entire assembly was then resealed and transferred to an optical bench for irradiation. The laser beam, collimated with a Pyrex iris, was passed coaxially through the cell. The power of the beam entering and leaving the cell was measured, and beam cross-section imprints were recorded. The valve to one of the collection compartments was then opened and the bottom of the compartment immersed in liquid nitrogen. Last, the valve to the sample reservoir (maintained at 25–26 °C) was opened and gaseous $U(OCH_3)_6$ allowed to pass through the irradiation area and into the cooled collection compartment. After 0.3–0.5 mg of red-orange material had been collected, the valve from the sample reservoir was closed, and after allowing several additional minutes for collection of residual material, the valve to the collection compartment was closed as well. The laser was adjusted to change output energy, and the process repeated by using an empty collection compartment. A total of three samples plus one reference sample were thus obtained. All of the aforementioned operations were carried out in subdued light to avoid possible UV–visible photolysis of the sample as it passed through the cell.

Isotopic Analysis. Mass spectrometry was conducted with a Hewlett-Packard 5985A instrument (several initial studies were conducted

(34) Sawyer, C. B. *J. Org. Chem.* **1972**, *37*, 4225.

with a Hewlett-Packard 5930A instrument[24a]) and attendant data system. The sample collection carousel was connected to the instrument via a 19/38 standard taper female joint and a tubular sample inlet (oven-dried overnight). This assembly interfaced to the spectrometer high-vacuum system via the direct injection port (DIP) of the spectrometer. Prior to sample introduction, a vacuum of 10^{-7} torr was maintained for 30 min or more, thus decreasing the possible loss of $U(OCH_3)_6$ reference material due to reaction with water adsorbed on the probe surfaces. The reference sample compartment (unirradiated $U(OCH_3)_6$) was next opened and sample vapor passed into the spectrometer. The tetramethoxyuranium(V) fragment ion, $U(OCH_3)_4^+$, was monitored at m/e 362.1 (70-eV ionizing voltage). The instrument was next tuned, optimizing the m/e 362.1 signal, so as to give an intensity of 1500–7000 counts/scan on maximum gain. Each scan was an average of eight measurements. Data were collected for 8 min, between m/e 355.0 and 365.0, at m/e 0.125 increments, resulting in the accumulation of ca. 1200 scans. Data from identical scans were averaged for peaks M − 3 (^{235}U), M + 1 (^{13}C), and M + 2 (^{18}O), where M represents the molecular mass of the species $^{238}U(^{16}O^{12}C^1H_3)_4^+$, to determine isotopic ratios in the standard (unirradiated) material. In addition, M − 4 and M − 5 peaks were also examined for use as base lines. This measurement procedure, with the exception of conditioning time and tune up, was repeated until the reading for the reference ^{235}U percentage had stabilized to within ±0.005% absolute. The actual instrumental error per scan is specified by the manufacturer at ±1% due to A/D converter roundoff. Thus, with assumption of random error, the absolute error should be on the order of ±0.0005%. This was not always obtainable due to slight but nonnegligible instrumental drift. Nevertheless, the measured isotopic enrichments were well beyond these uncertainties (vide infra).

When the requisite stability in isotopic composition was obtained for three consecutive reference (unirradiated) samples of $U(OCH_3)_6$, the first irradiated sample was analyzed by the same procedure, with the following additional guidelines: (i) No further tuning changes were made. (ii) The ion count was monitored to ensure residual $U(OCH_3)_6$ from the previous sample was cleared from the instrument. (iii) The entrance time of the sample was reduced to under 1 min in the already conditioned DIP probe assembly. An analysis procedure of alternating sample and reference measurements was employed. Each sample was compared to the reference immediately preceding and following it, and the enrichment factor and scatter limits were established for each sample individually. This methodology was found to be more accurate than use of the average of all references, as there was nonnegligible spectrometer drift over a 6-h period (typical measurement time per carousel). It was occasionally necessary to reject more than half of the experimental data as inconclusive because the drift rate was approximately equal to the change resulting from irradiation. A stable rate of sample flow was required to prevent an unequal weighting of the sequentially scanned masses. Enrichment measurements were conducted on $U(OCH_3)_6$ samples prepared from both natural and enriched (1.5% ^{235}U) uranium. The results were in good agreement.

Selectivity Measurements. The sample irradiation cell and associated components were scrupulously cleaned with dilute nitric acid, removing any trace of uranium oxides deposited on the walls or in the carousel. The cell conditioning procedure (vide supra) was then carried out in the irradiation area to allow complete thermal equilibrium to be established. Thereafter, three aliquots of $U(OCH_3)_6$ were passed through the cell and collected (3.0-h collection times each) in each of the three remaining compartments of the carousel. The second of these aliquots was collected while being irradiated by the laser at a frequency and power level giving a known enrichment of isotope ^{235}U (P(42)/3.2 J/cm^2). The uranium content of the collected samples was analyzed by a published spectrophotometric procedure.[35] Each of the collected samples was dissolved in 2.0 mL of 10^{-2} M HNO_3, and the pH was adjusted to ca. 7 with ethanolic KOH. Complexation was with 1.0 mL of 1% dibenzoylmethane (ethanol solution). The final volume of the solution was then adjusted to 50.00 mL with ethanol. The uranium concentration of the two unirradiated aliquots was compared to that of the irradiated one by measuring the optical absorption at 440 nm with a Cary 17D UV–visible spectrophotometer and correcting with a blank consisting of HNO_3 + KOH + dibenzoylmethane in ethanol.

Identification of Photolysis Products. Identification of the $U(OCH_3)_6$ dissociation products was conducted by irradiation at 1049 cm^{-1} (P(18) of the 9.6-μm branch) in a carefully cleaned cell. Total sample dissociation occurred at this wavelength, as judged by the lack of any observable collection of colored material in the cooled collection compartment. Irradiation for 8–9 h resulted in the formation of a cloudy tan film on the glass cell walls. In addition, brown material was noted on the inner surfaces of the cell windows at the edge of the area swept out by the laser beam, and colorless material condensed in the collection compartment. The cell was next transferred to the glovebox, where the windows were replaced with fresh KBr windows. The cell was then removed and evacuated to 10^{-4}–10^{-5} torr. With gentle heating from a heat gun, the tan material on the cell walls was slowly sublimed onto the inner faces of the fresh KBr windows. The cell was next returned to the glovebox, where the windows were removed, coated on the inner side with a drop of Nujol, and sandwiched together in a holder for infrared spectroscopy. The colorless material condensed in the 77 K collection compartment during photolysis was analyzed by mass spectrometry. Fragmentation patterns were compared to those of a variety of chemical compounds that were considered to be likely photolysis products.

Results

At the outset of this investigation, uranium alkoxides (known since the Manhattan Project)[37] were selected for study because of expected volatility, the inherent chemical flexibility of the U(V)–OR and U(VI)–OR frameworks, and the anticipation that uranium–ligand stretching fundamentals would occur in the 400–500-cm^{-1} region, giving rise to metal isotope sensitive overtones and combinations in the 800–1000-cm^{-1} region.[23] We begin with a discussion of $U(OCH_3)_6$ chemistry, volatility, and vibrational spectroscopy and then focus on the infrared photochemistry and isotope selectivity.

Uranium Hexamethoxide. Synthesis and Properties. Uranium hexamethoxide was originally synthesized by Gilman et al.[37] using the laborious, low-yield pathway indicated in eq 2–7. Alternative

$$UCl_4 + 4NaOC_2H_5 \rightarrow U(OC_2H_5)_4 + 4NaCl \quad (2)$$

$$U(OC_2H_5)_4 + {}^1/_2Br_2 \rightarrow U(OC_2H_5)_4Br \quad (3)$$

$$U(OC_2H_5)_4Br + NaOCH_3 \rightarrow U(OC_2H_5)_5 + NaBr \quad (4)$$

$$U(OC_2H_5)_5 + NaOC_2H_5 \rightarrow Na^+U(OC_2H_5)_6^- \quad (5)$$

$$Na^+U(OC_2H_5)_6^- + {}^1/_2[C_6H_5CO_2]_2 \rightarrow U(OC_2H_5)_6 + C_6H_5C^-O_2Na^+ \quad (6)$$

$$U(OC_2H_5)_6 + 6CH_3OH \rightarrow U(OCH_3)_6 + 6C_2H_5OH \quad (7)$$

syntheses were therefore developed that could produce large quantities of uranium hexamethoxide in greater yield and fewer steps. As outlined in the Experimental Section, $U(OCH_3)_6$ can be prepared in good yield from uranium tetrachloride via the approach of eq 8 and 9. Alternatively, efficient syntheses have

$$UCl_4 + 6LiOCH_3 \rightarrow Li_2U(OCH_3)_6 + 4LiCl \quad (8)$$

$$Li_2U(OCH_3)_6 + Pb(O_2CCH_3)_4 \rightarrow U(OCH_3)_6 + 2LiO_2CCH_3 + Pb(O_2CCH_3)_2 \quad (9)$$

also been developed that begin with UF_6 (eq 10 and 11).[29]

$$UF_6 + 2CH_3Si(OCH_3)_3 \rightarrow U(OCH_3)_6 + 2CH_3SiF_3 \quad (10)$$

$$UF_6 + 6NaOCH_3 \rightarrow U(OCH_3)_6 + 6NaF \quad (11)$$

Uranium hexamethoxide is a dark-red, moisture-sensitive, crystalline substance that sublimes readily at 30 °C (10^{-5} torr). It is soluble in most nonpolar organic solvents and is monomeric in benzene.[29] Uranium hexamethoxide appears to be slightly sensitive to visible or UV light and is best stored in the dark.

The solid-state molecular structure of uranium hexamethoxide has been determined by single-crystal X-ray diffraction, and the result is presented in Figure 2. The immediate coordination geometry about the uranium atom is essentially octahedral; however, the nonlinearity (ca. 160°) of the U–O–C vectors imparts an actual molecular symmetry of C_i in the solid state (neglecting the hydrogen atoms). The details of the molecular structure will be discussed elsewhere.[30] The vibrational spectroscopic data are

(35) Sandell, E. B. "Colorimetric Determination of Trace Metals"; Interscience: New York, 1959; Vol. 3, pp 918–919.

(36) (a) Bradley, D. C.; Mehrotra, R. C.; Gaur, D. P. "Metal Alkoxides"; Academic Press: New York, 1978. (b) Bradley, D. C. *Adv. Inorg. Chem. Radiochem.* **1972**, *15*, 259. (c) Bradley, D. C.; Fisher, K. J. *MTP Int. Rev. Sci.: Inorg. Chem., Ser. One* **1972**, *5*, 65.

(37) Jones, R. G.; Bindschadler, E.; Blume, D.; Karmas, G.; Martin, G. A., Jr.; Thirtle, J. R.; Yoeman, F. A.; Gilman, H. *J. Am. Chem. Soc.* **1956**, *78*, 6030.

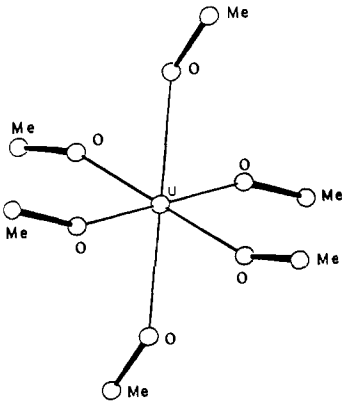

Figure 2. Solid-state molecular structure of $U(OCH_3)_6$ from ref 30.

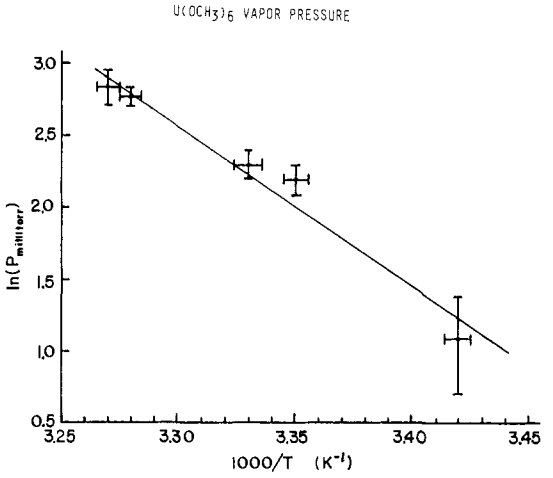

Figure 3. Vapor pressure of $U(OCH_3)_6$, plotted as ln P(mtorr) vs. $1/T$. The line represents the least-squares fit to the data (eq 12).

Table I. Heat of Sublimation and Entropy of Sublimation of Several Uranium Complexes

compd	$\Delta H_{sub}°$, kcal/mol	$\Delta S_{sub}°$, eu
$U(OCH_3)_6$	23 ± 3	76 ± 4
UF_6	12.0 ± 0.1[a]	40.0 ± 0.41[a]
$U(BH_4)_4$	19.5 ± 0.2[b]	61.2 ± 1.4[b]
$UO_2(HFA)_2 \cdot THF$[c]	14.0[d]	38[e]
$UO_2(HFA)_2$	35.1 ± 1.0[f]	89[g]
$UO_2(THD)_2$[h]	30.1 ± 2.1[f]	68[g]

[a] Calculated from data in ref 39. [b] Calculated from data in ref 27a. [c] HFA = hexafluoroacetylacetonate, $(CF_3CO)_2CH^-$; THF = tetrahydrofuran. [d] Taken from ref 40. [e] Calculated from graphical data in ref 40. [f] Taken from ref 26c. [g] Calculated from ref 26c, eq 1. [h] THD = 2,2,6,6-tetramethyl-3,5-heptanedionate.

in excellent accord with the near octahedral structure (vide infra).

Uranium Hexamethoxide. Vapor Pressure. The vapor pressure of $U(OCH_3)_6$ was measured at several temperatures from 19 to 33 °C. The data can be fit (correlation coefficient = 0.985) by a simple linear least-squares analysis to eq 12, which is plotted

$$\ln P(\text{mtorr}) = (38 \pm 17) - (10.9 \pm 0.5) \times 10^3/T \quad (12)$$

in Figure 3. The values $\Delta H_{sub}° = 23 \pm 3$ kcal/mol[38] and $\Delta S_{sub}° = 76 \pm 4$ eu[38] are found for the heat of sublimation and entropy of sublimation of $U(OCH_3)_6$, respectively, where standard deviations (3σ is quoted) are derived from the fitting procedure. Vapor pressure data for other volatile metal hexaalkoxides are not available for comparison;[36] however, values of $\Delta H_{sub}°$ and $\Delta S_{sub}°$ of some other volatile uranium complexes[26c,27a,39,40] are compiled in Table I.

(38) The values of $\Delta H_{sub}°$ and $\Delta S_{sub}°$ were derived from the Clapeyron equation

$$dP/dT = (\Delta H_{sub}°)(P)/RT^2 = (\Delta S_{sub}°)(P)/RT$$

Hence, $\Delta H_{sub}°/R$ is the slope of a plot of ln P vs. $1/T$ and $\Delta S_{sub}°/R$ the slope of a plot of ln P vs. ln T: Klotz, I. M.; Rosenberg, R. M. "Chemical thermodynamics", 3rd ed.; W. A. Benjamin: Menlo Park, CA, 1972; pp 160–162.

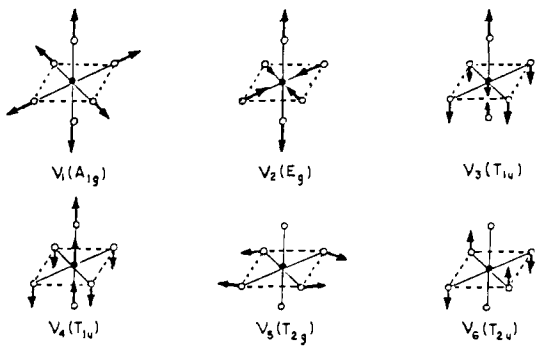

Figure 4. Normal modes of vibration for an octahedral MX_6 molecule.

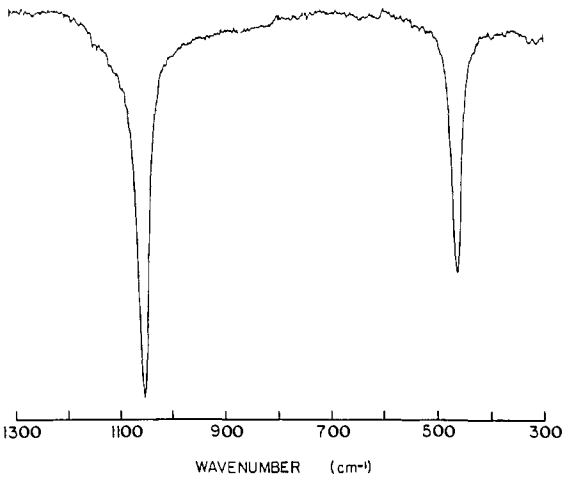

Figure 5. Infrared spectrum of a Nujol solution of $U(^{16}OCH_3)_6$.

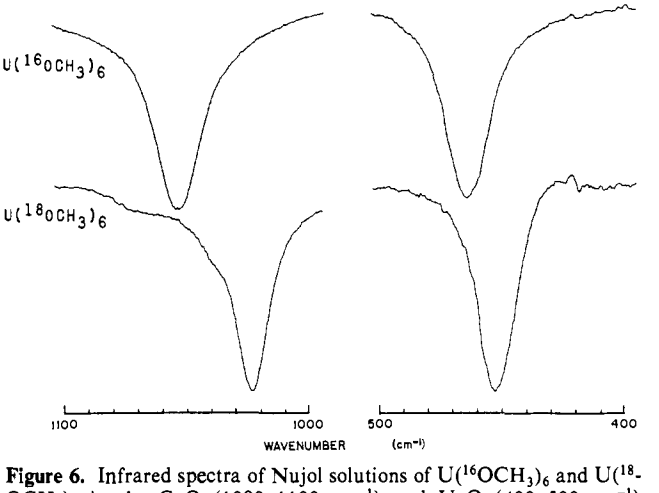

Figure 6. Infrared spectra of Nujol solutions of $U(^{16}OCH_3)_6$ and $U(^{18}OCH_3)_6$ in the C–O (1000–1100 cm^{-1}) and U–O (400–500 cm^{-1}) stretching regions.

Uranium Hexamethoxide. Vibrational Spectra. The normal modes of vibration for an octahedral MX_6 molecule are illustrated in Figure 4, and spectral activities are set out in Table II. As already noted, the UO_6 framework of $U(OCH_3)_6$ is of essentially octahedral symmetry. We now show that the observed $U(OCH_3)_6$ fundamental mode vibrational spectra (infrared and Raman) can

(39) Weinstock, B.; Crist. R. H. *J. Chem. Phys.* **1948**, *16*, 436.
(40) Kramer, G. M.; Dines, M. B.; Hall, R. B.; Kaldor, A.; Jacobson, A. J.; Scanlon, J. C. *Inorg. Chem.* **1980**, *19*, 1340.

Table II. Vibrational Spectroscopic Data for $U(OCH_3)_6$ and UF_6

type of internal coordinate change	sym type[a]	spectral activity	$^{238}U(^{16}OCH_3)_6$, cm^{-1} [b]			$^{238}U(^{18}OCH_3)_6$, cm^{-1} [b]		$^{238}UF_6$,	
			solid	solution	gas	solid	solution	cm^{-1} [c] gas	intensity
U–X stretch (ν_1)	A_{1g}	R	495.5	505.0		481.0		666.2	100[d]
U–X stretch (ν_3)	T_{1u}	IR	451.0	464.8	463.0		450.4	625.5	2000[e]
U–X stretch (ν_2)	E_g	R	400.6	414.0		386.0		533.4	8[d]
U–X deformation (ν_4)	T_{1u}	IR						186.2	100[e]
U–X deformation (ν_5)	T_{2g}	R						200.3	8[d]
C–O stretch	A_{1g}, T_{1u}, E_g	IR, R	1040	1051.5			1021.4		
U–X stretching combination ($\nu_1 + \nu_3$)	T_{1u}	IR						1290.9	4.1[e]
U–X stretching combination ($\nu_2 + \nu_3$)	T_{1u}, T_{2u}	IR						1156.9	4.7[e]

[a] Assuming local O_h symmetry. [b] All frequencies, unless otherwise specified, have an estimated accuracy of ±1.0 cm^{-1}. [c] Data of ref 20c; estimated accuracy ±0.5–1.0 cm^{-1}. [d] Data for UF_6.[20c] Relative intensities of Raman transitions. [e] Data for UF_6.[20c] Relative intensities (absorptivities) of infrared transitions. Intensities of infrared and Raman data cannot be compared.

be readily assigned under idealized O_h symmetry and by analogy to those of UF_6[20] and other octahedral MX_6[41] complexes. Although most of the present $U(OCH_3)_6$ data have not been obtained in the gas phase, those that have been obtained (vide infra) lend credence to the physically reasonable assumption that energies of vibrational bands in the gas phase and in noncoordinating, nonpolar solvents should be very similar. The infrared spectrum of a Nujol solution of $U(OCH_3)_6$ (Figure 5) exhibits two strong transitions at 1051.5 and 464.8 cm^{-1}, which shift to 1021.4 and 450.4 cm^{-1}, respectively, upon $^{18}OCH_3$ substitution (Figure 6). The high-energy absorption is assigned to modes that are predominantly ligand C–O stretching in character.[36,42,43] Under idealized O_h symmetry, the low-energy absorption is assigned to the highest frequency infrared-active, predominantly U–O stretching mode,[44] the ν_3 (T_{1u}) vibration. A significant harmonic oscillator, point mass (energy factored) calculation predicts a shift of 12.6 cm^{-1} in ν_{U-O} for proceeding from a simple $^{238}U-^{16}OCH_3$ to $^{238}U-^{18}OCH_3$ moiety, while a shift of 14.4 cm^{-1} is observed. In Nujol-free spectra of thin $U(OCH_3)_6$ films, ν_{C-O} and ν_3 U–O are observed at slightly lower energies, 1040 and 450 cm^{-1}, respectively. Gas-phase spectra of $U(OCH_3)_6$ could not be obtained in the C–O stretching region. Only broad absorptions at 1057 and 1015 cm^{-1} and a sharp absorption at 1034 cm^{-1}, all attributable to the ν_4 C–O stretch of gaseous CH_3OH,[45] were observed to grow over a period of several hours. It should be noted that these results do not invalidate or contradict the vapor pressure measurements on $U(OCH_3)_6$, in that the latter measurements were taken on a time scale of minutes, over which significant decomposition does not occur. A weak absorption not present in gaseous CH_3OH (transmittance = 99.4%[46]) was observed at 463 ± 1 cm^{-1}. This is tentatively assigned to the ν_3 U–O stretch of gaseous $U(OCH_3)_6$. Experiments with a longer path length cell are now in progress.

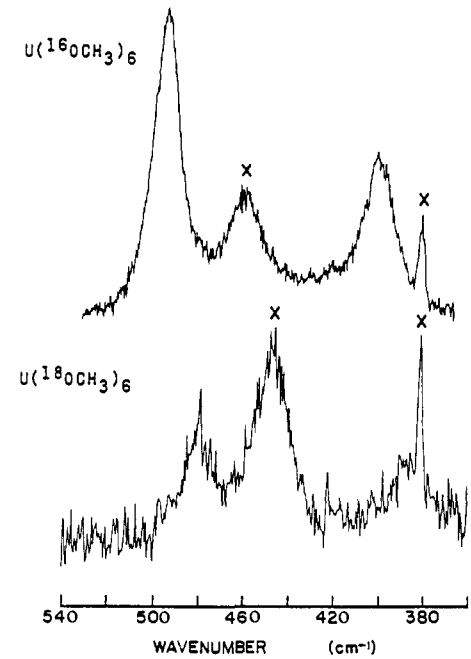

Figure 7. Laser Raman spectra (ν_0 = 6471 Å) of polycrystalline samples of $U(^{16}OCH_3)_6$ and $U(^{18}OCH_3)_6$ in the U–O stretching region. × denotes a decomposition product (higher frequency peak) and a laser plasma line (sharp, lower frequency emission).

The Raman spectra of polycrystalline $U(^{16}OCH_3)_6$ and $U(^{18}OCH_3)_6$ are shown in Figure 7. $U(^{16}OCH_3)_6$ exhibits two absorptions which are assigned, by analogy to UF_6 and other MX_6 molecules, to the ν_1 (A_{1g}) vibration at 495.5 cm^{-1} and to the ν_2 (E_g) vibration at 400.6 cm^{-1}. These absorptions shift to 481.0 and 386.0 cm^{-1}, respectively, upon $^{18}OCH_3$ substitution. Neither of these modes appears in the infrared spectra of the molecules, and likewise the infrared-active T_{1u} mode is not observed in Raman spectra. Thus, the exclusion rule is obeyed for this essentially octahedral system. The $U(^{16}OCH_3)_6$ ν_1 and ν_2 vibrations shift to slightly higher energy in toluene solution, i.e., to 505 and 414 cm^{-1}, respectively. The signal-to-noise ratio was not sufficient in solution Raman spectra to perform accurate depolarization measurements. The other spectroscopically active U–O modes (ν_4 and ν_5) are expected[20] to be weak, largely bending in character, and at lower energies than ν_1, ν_2, and ν_3. They have not been observed to date. No significant methoxy ligand vibrations are expected in the 400–500-cm^{-1} region.[36,42,43] Vibrational spectroscopic data for $U(OCH_3)_6$ fundamental modes are summarized and compared to the corresponding UF_6 assignments in Table II.

The $\nu_1 + \nu_3$ and $\nu_2 + \nu_3$ modes are among the most intense combination bands in the infrared spectrum of UF_6[20] and of other octahedral metal hexafluorides.[41] By analogy, a Nujol solution

(41) (a) Nakamoto, K. "Infrared and Raman Spectra of Inorganic and Coordination Compounds", 3rd ed.; Wiley-Interscience: New York, 1978; Chapter II-8. (b) McDowell, R. S.; Asprey, L. B. *J. Mol. Spectrosc.* **1973**, *48*, 254. (c) Weinstock, B.; Claassen, H. H.; Chernick, C. L. *J. Chem. Phys.* **1963**, *38*, 1470 and references therein.

(42) Adams, R. W.; Martin, R. L.; Winter, G. *Aust. J. Chem.* **1967**, *20*, 773.

(43) (a) Alpert, N. L.; Keiser, W. E.; Szymanski, H. A. "IR-Theory and Practice of Infrared Spectroscopy"; Plenum Press: New York, 1970; Chapter 5.10. (b) Bellamy, L. J. "The Infrared Spectra of Complex Molecules", 3rd ed.; Chapman and Hall: London, 1976; Chapters 6 and 7. (c) Socrates, G. "Infrared Characteristic Group Frequencies"; Wiley: Chichester, 1980; Chapters 2 and 7.

(44) (a) Ferraro, J. R. "Low Frequency Vibrations of Inorganic and Coordination Compounds"; Plenum Press: New York, 1971; Chapter 5. (b) Reference 41a, Chapters III-6 and IV-4.

(45) Serrallach, A.; Meyer, R.; Günthard, H. H. *J. Mol. Spectrosc.* **1974**, *52*, 94.

(46) The transmittance of the U–O ν_3 stretch in Figure 5, ca. 50%, arises from a Nujol solution containing ca. 2.4 μmol of $U(OCH_3)_6$. The vapor pressure of $U(OCH_3)_6$ at 27 °C is 0.01 torr, so the gas cell contains ca. 0.035 μmol of $U(OCH_3)_6$ vapor. The cross section of the solution cell is approximately 0.7 times that of the gas cell, so the calculated transmittance of the ν_3 band in the gas phase is given by

$$\log T_g = (0.7 m_g/m_s) \log T_s$$

where m_g = moles $U(OCH_3)_6$ in the gas phase, m_s = moles in the solution phase. Thus, T_g = 99.3%, close to the observed value.

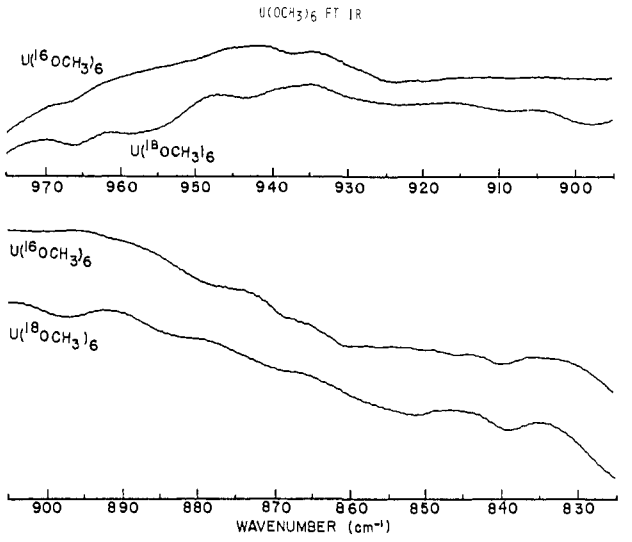

Figure 8. Fourier transform infrared spectra of Nujol solutions of $U(^{16}OCH_3)_6$ and $U(^{18}OCH_3)_6$ in the U–O $\nu_1 + \nu_3$ and $\nu_2 + \nu_3$ combination band region: 200 scans at 1-cm^{-1} resolution; Nujol subtraction and a five-point smoothing algorithm were applied; the $\%T$ scale is expanded to approximately 30 times that in Figure 5, the $\%T$ of the larger absorptions being approximately 0.26% that of the C–O stretch in Figure 5.

of $U(^{16}OCH_3)_6$ might be expected to exhibit nonnegligible U–O $\nu_1 + \nu_3$ and $\nu_2 + \nu_3$ absorptions at approximately 970 (in the 10-μm region) and 879 cm^{-1}, respectively. These absorptions should shift approximately 29 cm^{-1} to lower energy on $^{18}OCH_3$ substitution. Typical results of extensive Fourier averaging over the 825–975-cm^{-1} region of both $U(^{16}OCH_3)_6$ and $U(^{18}OCH_3)_6$ are presented in Figure 8. It can be seen that there are weak absorptions in the predicted regions (967 and 878 cm^{-1}) that shift approximately the requisite energy upon ^{18}O substitution (to 943 and 852 cm^{-1}, respectively). By analogy to UF_6,[20] these transitions are of approximately the correct intensity for $\nu_1 + \nu_3$ and $\nu_2 + \nu_3$[47] although they are also near the detection limit of the instrumentation. Strong absorptions in the wings of the C–O stretching fundamental preclude the use of more concentrated Nujol solutions or mulls.

Figure 8 also reveals two absorptions at 937 and 925 cm^{-1} in $U(^{16}OCH_3)_6$ which shift to 910 and 898 cm^{-1} in $U(^{18}OCH_3)_6$. In regard to understanding all of the $U(OCH_3)_6$ transitions in the 900–1000-cm^{-1} region and in view of the frequency dependence of the photochemical results (vide infra), it is important to consider how the origins and energies of spectral features in this region might be influenced by sample decomposition, anharmonicity, Fermi resonance, and distortion from idealized O_h symmetry.

Upon limited air exposure, a decomposition product appears at 928 cm^{-1} in the infrared spectrum of both $U(^{16}OCH_3)_6$ and $U(^{18}OCH_3)_6$. This is presumably a uranyl (UO_2^{2+}) compound,[40,48,49] possibly $UO_2(OCH_3)_2$, arising from partial $H_2{}^{16}O$ hydrolysis. Another absorption appears at 920 cm^{-1} on further air exposure, which can be assigned to monoclinic γ-UO_3.[50]

Possible thermal or photochemical $U^{16}O^{18}O^{2+}$- or $U^{18}O_2{}^{2+}$-containing decomposition products would be expected to absorb in the ranges 911–918 and 882–892 cm^{-1},[40] respectively, assuming the analogous $U^{16}O_2{}^{2+}$-containing product absorbs at 928 cm^{-1}. There may be a weak absorption at 884 cm^{-1} in the infrared spectrum of $U(^{18}OCH_3)_6$ (Figure 8). Therefore, it is conceivable that an absorption at 925 cm^{-1} in $U(^{16}OCH_3)_6$ could arise from thermal or photochemical decomposition. However, this seems doubtful since there is other evidence (vide infra) that $U(OCH_3)_5$, which does not have a major transition at 925 cm^{-1}, is the major photochemical decomposition product of $U(OCH_3)_6$. Decomposition products containing the $U{=}{}^{16}O$[51,52] or the $U{=}{}^{18}O$[51] group would be expected to absorb near 890 and 840 cm^{-1}, respectively.

In regard to assignments of U–O stretching combination bands and overtones in the 900–1000-cm^{-1} region (the 937- and 925-cm^{-1} transitions in particular), there is little indication that anharmonicity or Fermi resonance effects will be large. Although no relevant data for metal alkoxides are available, anharmonic corrections for metal–ligand stretching modes in octahedral metal fluorides[20,41] and carbonyls[53] are seldom greater than 6–8 cm^{-1} and are usually 0–3 cm^{-1}.[54a] Uranium hexafluoride[20] falls into the latter category. Thus, to assign the 937-cm^{-1} transition in $U(^{16}OCH_3)_6$ to $\nu_1 + \nu_3$ (970 cm^{-1} calculated from the fundamentals) would require an unusually large[54b-d] anharmonicity. Likewise, judging from the observed frequency separations as well as from data for metal hexafluorides,[20,31] it seems unlikely that Fermi resonance (e.g., the U–O stretching $\nu_1 + \nu_3$ (T_{1u}) combination interacting with the T_{1u} component of the C–O stretch) is important in determining the energies of the combination band transitions. For example, Fermi resonance interactions have been sought between combination bands or overtones and the ν_3 stretch in UF_6 and WF_6. In UF_6, the $\nu_2 + \nu_6$ combination band ($T_{1u} + T_{2u}$), located at 677 cm^{-1}, is the most intense combination band in the UF_6 spectrum.[20] A Fermi resonance interaction of the $\nu_2 + \nu_6$ band with the ν_3 stretch at 625.5 cm^{-1} was previously postulated[41c] to account for this. However, on the basis of improved spectroscopic data,[20c] it now appears that any interaction must be slight since the predicted position of $\nu_2 + \nu_6$ is 676 ± 2 cm^{-1}, as observed. In WF_6,[41b] the ν_3 stretch is located at 712 cm^{-1}. The $\nu_2 + \nu_6$ combination band, which again is relatively strong, is located at the predicted position of 808 cm^{-1}. The weak $3\nu_4$ overtone of WF_6 (which contains a T_{1u} component) is located at 745 cm^{-1}, also near the predicted position of 753–759 cm^{-1} (ν_4 252 ± 1 cm^{-1}). It therefore seems unlikely that the $U(^{16}OCH_3)_6$ $\nu_1 + \nu_3$ combination band, expected 80 cm^{-1} lower in energy than the C–O stretch, would undergo an interaction strong enough to displace it to the ca. 930-cm^{-1} region.

It is difficult to predict the exact spectral consequences in the 900–1000-cm^{-1} region of small departures from idealized O_h symmetry. Although departure from centrosymmetric symmetry (the crystallographic symmetry is centrosymmetric, C_i) would, in principle, lend infrared spectral activity to $2\nu_2$ (ca. 828 cm^{-1}), $\nu_1 + \nu_2$ (ca. 919 cm^{-1}), $2\nu_3$ (930 cm^{-1}), and $2\nu_1$ (1010 cm^{-1}), firm evidence for such a departure is not evident in the activity of the

(47) On the basis of the relative absorptivities, a, of the infrared vibrations in UF_6 (ref 20c), Beer's law was used to calculate the anticipated percent transmittance, T, of the $\nu_1 + \nu_3$ and $\nu_2 + \nu_3$ combination bands (cb) for a spectrum such as that in Figure 8, where the transmittance of the U–O ν_3 stretch is approximately 50%.

$$\log T_{cb} = (a_{cb}/a_{\nu_3}) \log T_{\nu_3}$$

This calculation predicts the transmittance of the $\nu_1 + \nu_3$ and $\nu_2 + \nu_3$ combination bands to be approximately 99.86%, 0.28% as intense as ν_3.

(48) The UO_2^{2+} antisymmetric stretch in uranyl compounds is found typically between 860 and 960 cm^{-1}: Casellato, U.; Vidali, M.; Vigato, P. A. *Inorg. Chim. Acta* **1976**, *18*, 77.

(49) (a) Jones, L. H. *J. Opt. Soc. Am.* **1964**, *54*, 1283. (b) Kharitonov, Y. Y.; Buslaev, Y. A. *Opt. Spectrosc. (Engl. Transl.)* **1963**, *14*, 311.

(50) Roman, W. C. "United Technologies Research Center Report"; United Technologies: East Hartford, CT, 1976; R76-912205, Figure 84c. We thank Dr. Roman for a copy of this report.

(51) Jacob, E.; Polligkeit, W. *Z. Naturforsch.* **1973**, *28*, 120.

(52) Paine, R. T.; Ryan, R. R.; Asprey, L. B. *Inorg. Chem.* **1975**, *14*, 1113.

(53) Jones, L. H. McDowell, R. S.; Goldblatt, M. Inorg. *Chem.* **1969**, *8*, 2349.

(54) (a) On the basis of the observed fundamental transitions, true anharmonic shifts of the combination bands are obviously somewhat greater than this if the harmonic frequencies (ω_i) of the fundamentals are considered instead. For UF_6,[20d] $\omega_1 = 672 \pm 6$ cm^{-1} and $\omega_3 = 634 \pm 6$ cm^{-1}, therefore $\omega_1 + \omega_3 = 1306 \pm 12$ cm^{-1}. The observed frequency is $\nu_1 + \nu_3 = 1291 \pm 0.5$ cm^{-1}; the predicted frequency from the observed fundamentals is 1293 ± 2 cm^{-1}. Therefore, although the combination band is observed within 0–4 cm^{-1} of its calculated position, there is still an anharmonic shift of 3–27 cm^{-1} (0.2–2.1%). (b) To our knowledge, the 1.7% (13 cm^{-1}) shift in the $E_g + T_{1u}$ M–C stretching combination of $Mo(CO)_6$[54c] is the largest reported effect for a metal–ligand stretching mode.[53] (c) For an extensive compilation of anharmonicity data for diatomics, see ref 41a, p 106. (d) This qualititative discussion has neglected the effects of hot bands, which could not be ignored in a more rigorous description of the $U(OCH_3)_6$ force field. For a discussion of these problems in UF_6, see ref 20d.

fundamental transitions. Thus, the origin of the 937- and 925-cm^{-1} transitions in this complex molecule remains incompletely resolved. At present, assignments involving U–O stretching overtones and/or combinations under lowered symmetry or severe anharmonicity appear most plausible. Less plausible explanations include nonfundamental methoxy-centered transitions and/or difference transitions.[55]

In UF_6, the ^{235}U–^{238}U shift of ν_3 is reported to be 0.65 ± 0.1 cm^{-1},[20] while the shift for both $\nu_1 + \nu_3$ and $\nu_2 + \nu_3$ is 0.5 ± 0.1 cm^{-1}.[20a] These parameters were determined from infrared measurements on essentially isotopically pure $^{238}UF_6$ and $^{235}UF_6$ samples. Although samples of such high ^{235}U enrichment were not available for the present investigation, it is possible to make reasonable estimates of the ^{235}U–^{238}U shifts in $U(OCH_3)_6$ by several lines of argument. From the Teller–Redlich product rule (eq 13),[56] where m and M are atomic and molecular masses,

$$\frac{\nu_3\nu_4(^{238}U)}{\nu_3\nu_4(^{235}U)} = \left[\frac{m(^{235}U)}{m(^{238}U)}\,\frac{M(^{238}U(OCH_3)_6)}{M(^{235}U(OCH_3)_6)}\right]^{1/2} \quad (13)$$

respectively, the isotopic ratio of the T_{1u} modes is calculated to be 0.9972 (point mass approximation) vs. 0.9979 in UF_6. The same ratio is calculated to be 0.9982 for a bare UO_6 framework. Assuming the shift distribution between the bending and stretching modes is the same as in UF_6,[20d] the ^{235}U–^{238}U displacement in ν_3 is estimated to be ca. 0.88 cm^{-1} (point mass approximation) or ca. 0.42 cm^{-1} (UO_6 framework). An alternative approach to estimating the metal isotope shift is to use a first-order perturbation theory procedure,[57] together with the UF_6 data (eq 14). Thus,

$$\frac{\Delta\nu(UOCH_3)}{\Delta\nu(UF)} = \frac{[a\nu(UOCH_3)\Delta\mu_U/\mu_{OCH_3}]^{1/2}}{[a\nu(UF)\Delta\mu_U/\mu_F]^{1/2}} \quad (14)$$

for the T_{1u} mode, where a is a constant and the μ's are reciprocal masses, a shift in the $U(OCH_3)_6$ T_{1u} U–O stretching mode of ca. 0.72 (point mass approximation) or ca. 0.51 cm^{-1} (UO_6 approximation) is estimated. These results argue that ^{235}U–^{238}U isotopic shifts comparable to those found in UF_6 can be expected for the ν_3 fundamental as well as the $\nu_2 + \nu_3$ and $\nu_1 + \nu_3$ (10 μm) combination modes of $U(OCH_3)_6$. The shift for an overtone such as $2\nu_3$ should be approximately twice as large.

Laser-Induced Chemistry. The experiments involving infrared multiphoton absorption of $U(OCH_3)_6$ can be divided into two basic classes: (i) those designed to elucidate the fundamental mechanistic processes following infrared multiphoton absorption and (ii) those experiments related to the isotopic selectivity of the multiphoton absorption process. The first class of experiments was performed by irradiation of $U(OCH_3)_6$ with a line of the 9.6-μm CO_2 laser branch, which is in resonance with the C–O stretching fundamental of the methoxy ligand (1051.5 cm^{-1}). Since this ligand internal stretching vibration would not be expected to exhibit a significant uranium isotope shift, no isotopic selectivity would be anticipated in the dissociation process. The magnitude of the infrared absorption coefficient, as judged from the infrared spectrum of $U(OCH_3)_6$ in this region is significantly greater than the absorption coefficient in the region where isotopic enrichment has been observed (vide infra). For a number of medium-sized hydrocarbons with typically ~40 vibrational normal modes, good correlations have been observed between the magnitude of the normal infrared absorption cross section as taken from infrared spectra and the multiphoton absorption cross section.[58,59] Furthermore, multiphoton absorption cross sections in many systems remain constant as a function of fluence, implying an absorption cross section that does not significantly vary as a function of level of excitation.[58,59] In such systems, densities of states approach the criterion used for the onset of the quasi-continuum, ca. 100 states/cm^{-1}, near 3000 cm^{-1}, i.e., approximately the v = 3 level of the pumped mode.[59] Uranium hexamethoxide has 87 normal modes, many of which are of substantially lower frequency than in the aforementioned hydrocarbon systems. Thus, the assumption seems justified that $U(OCH_3)_6$ has a low-lying quasi-continuum and does not exhibit "bottlenecking" in the discrete region and that the multiphoton absorption cross section scales with the single-photon absorption cross section.

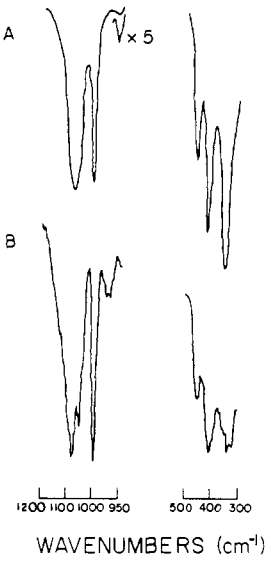

Figure 9. Infrared spectra of (A) $U(OCH_3)_5$ and (B) $U(OCH_3)_6$ infrared photolysis product. Spectra were recorded as thin films.

From the foregoing discussion it would be expected that at a given fluence, significantly more dissociation would be observed upon irradiation of the $U(OCH_3)_6$ C–O stretch than in the 900–1000-cm^{-1} region. This is observed as evidenced by the fact that under these conditions and at a fluence of ca. 3 J/cm^2, no uranium-containing products were observed in the collection vessel of the photolysis apparatus. However, during these photolysis experiments, the walls of the irradiation cell became coated with a tan solid that could be collected by low-temperature sublimation. As can be seen in Figure 9, the infrared spectrum of the photoproduct is essentially identical with that of an authentic sample of $U(OCH_3)_5$ (which is a tan solid of considerably lower vapor pressure than $U(OCH_3)_6$[60]). The simplest explanation for this result is a homolytic dissociation process (eq 15). Thermochemical

$$U(OCH_3)_6 \xrightarrow{h\nu} U(OCH_3)_5 + CH_3O\cdot \quad (15)$$

support for this reactivity mode is derived from the relatively low estimated $U(OCH_3)_6 \rightarrow U(OCH_3)_5$ U–O bond dissociation energy, ca. 60 kcal/mol.[61] Furthermore, substantial quantities of methanol and formaldehyde are detected as the organic photolysis

(55) In UF_6,[20c] the difference bands in the region of $\nu_1 + \nu_3$ and $\nu_2 + \nu_3$ are less intense than the combinations by several orders of magnitude.

(56) (a) Reference 41a, Chapter I–15. (b) Nakamoto, K. *Angew, Chem., Int. Ed., Engl.* **1972**, *11*, 666. (c) Herzberg, G. "Molecular Spectra and Molecular structure. Infrared and Raman Spectra of Polyatomic Molecules"; Van Nostrand, New York, 1956; Vol II, pp 231–238.

(57) (a) Mohan, N.; Müller, A.; Nakamoto, K. *Adv. Infrared Raman Spectrosc.* **1975**, *1*, 173. (b) Müller, A.; Schmidt, K. H.; Mohan, N. *J. Chem. Phys.* **1972**, *57*, 1752.

(58) Danen, W. C.; Tang, J. D. In "Laser-Induced Chemical Processes"; Steinfeld, J. I.; Ed.; Plenum Press: New York, 1981, Vol. 1, Chapter 2.

(59) Buechele, J. L.; Weitz, E.; Lewis, F. D. *J. Chem. Phys.* **1982**, *77*, 3500–3507.

(60) Miller, S. S. Ph.D. Thesis, Northwestern University, 1980.

(61) (a) This quantity was estimated by using the mean bond dissociation energy proportionalities where

$$U(OR)_6/UF_6 = U(OR)_5/UF_5 = U(OR)_4/UF_4 = Zr(OR)_4/ZrF_4$$

the metal fluoride and zirconium alkoxide (R = i-C_3H_7) data are from the literature.[61b-d] The $U(OCH_3)_6$ result can be compared to a value of 74 kcal/mol for UF_6. That an analogous treatment ($ZrCl_4/ZrF_4$) predicts the mean UCl_6 bond dissociation energy to within 4% of that obtained from thermochemical data supports the validity of the proportionality approximation. (b) Huheey, J. E. "Inorganic Chemistry", 2nd ed.; Harper and Row: New York, 1978; Appendix F. (c) Connor, J. A. *Top. Curr. Chem.* **1977**, *71*, 71. (d) Brown, D. In "Comprehensive Inorganic Chemistry"; Bailar, J. C., Emeleus, H. J., Nyholm, R. S., Trotman-Dickenson, A. F.; Eds.; Pergamon Press: Oxford, 1973; Vol. 5, p 155.

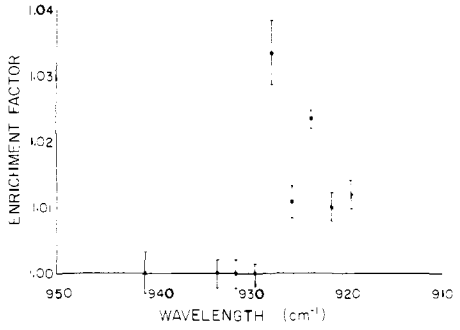

Figure 10. Laser wavelength dependence of the ^{235}U enrichment in $U(OCH_3)_6$ resulting from infrared photolysis. Each point represents the average of two to five measurements.

products, consistent with the established disproportionation pathway for methoxy radicals (eq 16).[62]

$$2CH_3O\cdot \rightarrow CH_3OH + CH_2O \qquad (16)$$

Other reactions leading to less volatile products could also occur and would not be readily detected due to the sublimation procedure used to collect photoproducts for infrared spectroscopy. For example, gaseous $U(OCH_3)_5$ is likely (depending upon the degree of association and whether there are bridging methoxy ligands present) to have relatively significant absorptions in the 900–1100-cm^{-1} region[36a] and, following production from $U(OCH_3)_6$, could absorb more photons and fragment further.

In a variety of infrared multiphoton excited systems, a product fluence dependence has been observed.[63] Often this fluence dependence occurs when reaction channels of nonidentical but similar activation energies are accessible to the excited parent. A high activation energy (E_a) channel can actually dominate a lower activation energy channel if the low activation energy channel also has a low preexponential factor relative to that of the high E_a channel. Under these circumstances high levels of excitation may lead to a relative favoring of the high E_a channel.[63] A priori, this could be a concern in the hexamethoxide system in that significantly higher levels of excitation are expected with the laser line in resonance with the C–O stretching mode. However, in general, competing unimolecular homolytic bond cleavage pathways would not be expected to have differences in preexponential factors that would allow them to make up for the expected large activation energy difference between energy fragmentation pathways. Thus it seems reasonable to conclude that the initial fundamental dissociative step in $U(OCH_3)_6$ is independent of excitation frequency.

Isotope-Selective Chemistry. Isotopically selective reactions were observed for five laser lines between 919 and 935 cm^{-1} with the largest separation factor being observed for the P(38) laser line of the 10.6-μm branch at 927 cm^{-1} (Figure 10). If isotopic enrichment, β, is formally defined as in eq 17, then in the present

$$\beta = (^{235}U/^{238}U)_{final}/(^{235}U/^{238}U)_{initial} \qquad (17)$$

system, the maximum enrichment observed was $\beta \approx 1.034$ (10) at a fluence of ca. 3.2 J/cm^2. As a check, these experiments were carried out with both natural uranium and uranium enriched to 1.5% in ^{235}U. Enrichment results scaled as expected within experimental error.

The fraction of $U(OCH_3)_6$ actually dissociated in a single pass through the irradiation cell was of great interest in assessing the actual efficiency of the isotope separation process. This was determined by condensing a $U(OCH_3)_6$ sample without the laser operating, repeating the process for the same period of time with the laser operating (collecting that material in a separate finger of the collection cell), and finally collecting another blank in a separate container. The amount of uranium present in each sample was determined spectrophotometrically. These results at a fluence level of ~4 J/cm^2 indicate that less than 10% of the $U(OCH_3)_6$ is dissociated in a single pass when irradiation is performed with the P(38) 9.6-μm laser wavelength. With an average enrichment factor of 1.034 (10) and less than 10% dissociation, this translates to a selectivity of greater than ca. 1.4, where the selectivity, α, is defined as in eq 18.[2] Here f is the fraction of material left

$$\alpha = \ln f/\ln (f\beta) \qquad (18)$$

undissociated and β is the aforementioned isotopic enrichment factor.

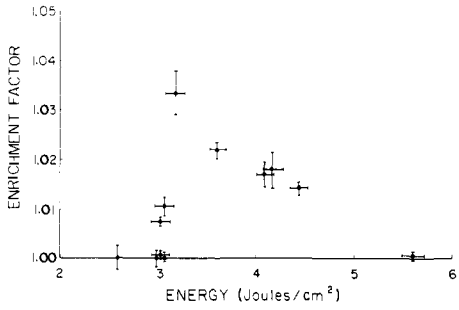

Figure 11. Fluence dependence of the ^{235}U enrichment in $U(OCH_3)_6$ when irradiating on the P(38) laser line.

The 927-cm^{-1} irradiation region is in close proximity to the predicted position of the $2\nu_3$ overtone of $U(OCH_3)_6$, which should be weakly active if there is a breakdown of the idealized octahedral molecular symmetry (vide supra). As indicated previously, this overtone should exhibit a significant uranium isotope shift (~1.0–1.5 cm^{-1}), and the source of uranium isotopic selectivity in the system is tentatively attributed to absorption in this band. However, to reiterate, it is also possible that the absorptions occurring in the region exhibiting isotope selectivity are due to highly anharmonic overtones or combinations, or to difference transitions which are isotopically sensitive.

Experiments involving the fluence dependence of the enrichment in ^{235}U were carried out for $U(OCH_3)_6$ irradiation with the P(38) laser line. The results are summarized in Figure 11. The expected behavior of the enrichment factor as a function of fluence can first be considered. Although it has been shown that for large molecules in collision-free situations there may be no fluence threshold for multiphoton dissociation,[64] a threshold for isotopically selective dissociation would be expected for the type of experiment discussed herein. Two primary factors would be expected to lead to a threshold on the low fluence side. First, in a "bulb" experiment, the laser must deliver a sufficient fluence so that uppumping can compete with collisional deactivation. Secondly, for the experiments herein, the undissociated material was collected and analyzed by mass spectral procedures. Under these circumstances, sufficient material must be dissociated in an isotopically selective fashion to result in a detectable change in isotope ratio in the remaining material. For the experiments reported, the latter factor is probably more important and results in an effective low fluence threshold to isotopic selective dissociation that appears at ~3 J/cm^2.

The high fluence limit involves a different situation and mechanism. In previous studies, a diminution in isotope selectivity has been postulated and observed as a function of increasing laser fluence.[65] In these studies the cause of the diminution in selectivity was postulated to be due to power broadening at high fluence causing an increase in the relative amount of dissociation of the unwanted isotopic material. The magnitude of this effect should increase as the isotopic splitting decreases, and the degree of power

(62) (a) Batt, L.; Burrows, J. P.; Robinson, G. N. *Chem. Phys. Lett.* **1981**, *78*, 467–470 and reference therein. (b) Batt, L.; Robinson, G. N. *Int. J. Chem. Kinet.* **1979**, *11*, 1045 and references therein. (c) Batt, L.; Rattray, G. N. *Ibid.* **1979**, *11*, 1183 and references therein. (d) Wiebe, H. A.; Heicklen, J. *J. Am. Soc.* **1973**, *95*, 1, 7. (e) Zaslonko, I. S.; Kogarko, S. M.; Mozzhukhin, E. V.; Petrov, Y. P.; Borisov, A. A. *Kinet. Katal.* **1970**, *11*, 296.

(63) (a) Buechele, J. L.; Weitz, E.; Lewis, F. D. *J. Am. Chem. Soc.*, in press. (b) Brenner, D. M. *Chem. Phys. Lett.* **1978**, *57*, 357. (c) Lussier, F. M.; Steinfeld, J. I. *Chem. Phys. Lett.* **1977**, *50*, 175.

(64) Bomse, D. S.; Woodin, R. L.; Beauchamp, J. L. "Advances in Laser Chemistry"; Zewail, A. H., Ed.; Springer-Verlag: Berlin, 1978; pp 362–373.

(65) (a) Mukamel, S.; Jortner, J. *J. Chem. Phys.* **1976**, *65*, 5207. (b) Hackett, P. A.; Willis, C.; Gauthier, M. *Ibid.* **1979**, *71*, 2682.

broadening is proportional to the Rabi frequency, which in turn is proportional to the product of the electric field strength and the dipole moment derivative matrix element.[66] At the fluences used in this study and from the estimated magnitude of the matrix element at the laser frequency, this term is too small to be the likely cause of the observed decrease in selectivity in the present system.

Another possible cause of decreased enrichment upon increasing fluence is chemical in nature. If the nonselective reaction of $U(OCH_3)_6$ with photoproducts increases as a function of fluence, then isotopic selectivity will decline. This could occur in a variety of ways. As previously indicated, gaseous $U(OCH_3)_5$ may exhibit significant absorption near the P(38) laser frequency. Thus the further fragmentation of $U(OCH_3)_5$ could increase as fluence increased. This secondary photolysis would result in the generation of increasing quantities of methoxy radicals with increasing fluence. These methoxy radicals would then be expected to react in a nonisotopic specific fashion with the remaining $U(OCH_3)_6$ plausibly abstracting a hydrogen atom to generate $U(OCH_3)_5$, CH_3OH, and H_2CO. The net effect of this process would be to diminish the total quantity of collected, enriched material. Bearing in mind that the present irradiation configuration dissociates only a small percentage of the $U(OCH_3)_6$ molecules, the dilution resulting from combined collection of irradiated and nonirradiated material could diminish the measured isotopic enrichment. Other processes that could occur that also would diminish the isotopic yield of product involve enhanced reactivity of vibrationally excited species. Though these are less likely sources of the observed effect since few demonstrable cases exist for vibrationally enhanced reactions,[67] they are mentioned for completeness. Reactions whose rate would be expected to increase with fluence and would nonspecifically destroy $U(OCH_3)_6$ include:

$$U(OCH_3)_5^* + U(OCH_3)_6 \rightarrow U(OCH_3)_6 + U(OCH_3)_5 \quad (19a)$$

$$U(OCH_3)_5^* + U(OCH_3)_6 \rightarrow 2U(OCH_3)_5 + \cdot OCH_3 \quad (19b)$$

where the asterisk represents a vibrationally excited species. In eq 19a the ligand-exchange reaction would actually be antispecific since the originally formed $U(OCH_3)_5$ is now returned to the gas phase. The degree of excitation in the $U(OCH_3)_5$ would be increased with fluence due to the strong absorption in the 10-μm region.

Thus we postulate (i) an increase in the dissociation probability of $U(OCH_3)_5$ coupled with the possibility of reactions similar to those of eq 19b and (ii) some influence due to power broadening as the source(s) of the diminished isotopic yield with increasing fluence for the $U(OCH_3)_6$ system.

Conclusions

The most immediate consequence of this study is the demonstration of significant uranium isotope separation upon gas-phase photolysis of $U(OCH_3)_6$ in a spectral region where isotope-sensitive U–O stretching overtone and combination transitions are expected. Although the basic aspects of both the $U(OCH_3)_6$ vibrational force field and multiphoton infrared photochemistry have been elucidated in the present study, certain physicochemical details, the nature of which is endemic to complex multiatom molecules, remain to be understood. In a technological sense, promising directions for improvement of yield and selectivity in isotope separation processes utilizing this compound include the use of scavengers, multilaser excitation, modification of the irradiation geometry, and the use of a supersonic expansion nozzle for cooling. Also promising is the design and refinement of other volatile uranium compounds for 10-μm isotope separation processes. A number of new molecular candidates are conceivable,[23,24] and the recent results with uranyl compounds[6,15] and uranium borodeuteride[28] confirm the attractiveness of such an approach.

Acknowledgment. We thank the National Science Foundation (T.J.M., Grant CHE8009060) and the Electric Power Research Institute (T.J.M., E.W., Contract RP506-7) for support of this research. Raman spectra were recorded in the Raman Facility of the Northwestern Materials Research Center, supported by the NSF–MRL program (Grant DMR79-23573); we are grateful to C. W. Dirk for assistance with these Raman spectra.

Registry No. $U(OCH_3)_6$, 69644-82-2; CCl_4, 10026-10-5; $Li_2(U(OCH_3)_6)$, 85735-25-7; $U(^{18}OCH_3)_6$, 83178-44-3; UF_6, 7783-81-5; $Na^{18}OCH_3$, 85735-26-8; ^{235}U, 15117-96-1; $HOCH_3$, 67-56-1; $U(OCH_3)_5$, 83178-45-4; formaldehyde, 50-00-0.

(66) See, for example, ref 2d,e.
(67) Kneba, M.; Wolfrum, J. *Annu. Rev. Phys. Chem.* 1980, 31, 47.